Aerosol and Air Quality Research, x: 1–11, xxxx

ISSN: 1680-8584 print / 2071-1409 online
doi: 10.4209/aaqr.2017.11.0473

Implication of Light Absorption Enhancement and Mixing State of Black Carbon (BC) by Coatings in Hong Kong

Guo-Liang Li[1], Li Sun[1], Kin-Fai Ho[2], Ka-Chun Wong[1], Zhi Ning[3*]

[1] *School of Energy and Environment, City University of Hong Kong, Hong Kong, China*
[2] *The Jockey Club School of Public Health and Primary Care, Chinese University of Hong Kong, Hong Kong, China*
[3] *Division of Environment and Sustainability, Hong Kong University of Science and Technology, Hong Kong, China*

ABSTRACT

Simultaneous measurements of black carbon (BC) and non-refractory PM_1 aerosol chemical compositions were performed in autumn 2016 at a suburban site in Hong Kong. A thermodenuder (TD) was employed at different heating temperatures to remove semi-volatile aerosol fractions to varying degrees. The light absorption enhancement (E_{abs}) of BC due to semi-volatile coatings at seven wavelengths was evaluated, and the coating fractions were further analyzed. Results showed that the overall E_{abs} ranged from 1.58 ± 0.13 (470 nm) to 1.64 ± 0.16 (660 nm) at 280°C and increased very little from 50°C (1.02–1.04) to 200°C (1.13–1.20). The lensing-effect-related E_{abs} was probably attributable to the presence of ammonium and sulfate. Furthermore, the ratio of the coating thickness to the BC core radius was around 1.0–2.0 based on Mie calculations. This work evaluated the E_{abs} from coatings in Hong Kong and implied the BC mixing state, thus providing a critical reference for climate models on the role of aerosol in global warming.

Keywords: Thermodenuder; BC coating; Mie calculation.

INTRODUCTION

Black carbon (BC) is one of the major components of $PM_{2.5}$ formed in flames during combustion of carbon-containing fuels, which often exists as an aggregate of small graphite spheres (Bond *et al*., 2013). In recent decades, BC has been an area of intensive research due to its positive effect on global radiative forcing scales. Especially in climatology, many academics regard BC as the second most important contributor to global warming after carbon dioxide (Jacobson 2001; IPCC 2007; Ramanathan and Carmichael, 2008; Srivastava *et al*., 2012).

One key factor that defines the BC contribution to radiative forcing is its mixing state with other aerosol components, e.g., external mixture, volume mixture and encapsulated mixture, of which the last one (also known as coating-core mixing) has been recognized as the most realistic scenario, since BC is a solid and cannot physically be well mixed in a particle (Jacobson, 2001; Bond and Bergstrom, 2006). In this case, so-called coating materials surrounding BC core could act as a lens and enhance light absorption through the "lensing effect" (Fuller *et al*., 1999). Many studies have assessed such light absorption enhancement (E_{abs}) based on theoretical estimation, lab experiment and field measurement. Jacobson (2001), Schnaiter *et al*. (2005) and Moffet and Prather (2009) calculated an E_{abs} of 1.6–2.0 compared to that of fresh BC spherules as core using core-shell Mie theory. Shiraiwa *et al*. (2010) experimentally observed an E_{abs} of 1.3 when coated by a small amount of organic coatings with shell/core diameter ratio of 1.2, but the E_{abs} reached as high as 2 with shell/core diameter ratio of 2. For E_{abs} of field measurement, Cappa *et al*. (2012) didn't observe such high value with E_{abs} of only ~1.1 in coastal California; while Lack and Schwarz (2012) and Liu *et al*. (2015) observed higher E_{abs}, with the value of 1.4 in Colorado, USA and 1.3–1.4 in Detling, UK, respectively.

The discrepancies of reported E_{abs} among field measurement, lab experiment and theoretical calculation raise concerns of uncertainty in evaluating the impact of BC on global radiative forcing budget. Liu *et al*. (2015) argued that the influence of coatings on light absorption is more of source- and region-dependent. Lack and Cappa (2010) pointed out that widely-used Mie model gives different results based on different assumptions that coatings are either non- or weakly absorbing especially in UV region, as is experimentally verified with weakly absorbing humic acid as coatings (You *et al*., 2016).

In this work, we evaluated the light absorption enhancement (E_{abs}) by field observation in Hong Kong, and performed further simulation using Mie model to inversely

* Corresponding author.
Tel.: 852-3469 2207
E-mail address: zhining@ust.hk

deduce coating thickness and relevant optical properties. A thermodenuder (TD) was designed and evaluated with good performance to volatilize semi-volatile coating materials and assess the E_{abs}. An Aerosol Chemical Speciation Monitor (ACSM) was also employed to characterize the semi-volatile coatings. This paper aims to: 1) evaluate E_{abs} by field observation in an urban area; 2) characterize BC mixing state (coating thickness, heterogeneity of light absorption for coating, etc.).

MATERIAL AND METHODS

The experiment was conducted at Air Quality Management System (AQMS) site of Hong Kong Environmental Protection Department, a suburban site in Hong Kong (Fig. S1), from Oct. 30, 2016, to Nov. 14, 2016. A schematic of the experimental setup is shown in Fig. 1. Ambient aerosols were sampled intermittently through thermodenuder (TD) set at different temperatures (50°C, 100°C, 150°C, 200°C and 280°C) and direct ambient sampling without TD every 10 minutes. Relative humidity (RH) was controlled at 20–30% with the Nafion drier, as it has significant impact on light absorption of BC (Cappa *et al*., 2012; Cheng *et al*., 2014). Measurement was conducted behind TD using an Aethalometer (AE33, Magee Scientific Corporation) for BC mass and light absorption determination at seven wavelengths (370 nm, 470 nm, 520 nm, 590 nm, 660 nm, 880 nm, 950 nm), and an Aerodyne Aerosol Chemical Speciation Monitor (ACSM) for sub-micron aerosol composition. Auto-valve control system and TD are homemade with its performance evaluated in the supplementary document.

Design of Thermodenuder

The design of the TD used in this study is based on Wehner *et al*. (2002) and Burtscher *et al*. (2001) with two tandem sections for heating and cooling (see Fig. 2). In the heating section, heating tape was twined evenly around a stainless steel (SS) tube with inner diameter (ID) of 22 mm, and then covered by a thermal insulation sleeve filled with thick glass fiber. In the cooling section, inner tube made of SS mesh allowed quick absorption of evaporated materials onto activated charcoal, surrounded with an air-cooled spiral copper tube (ID is 6 mm) to provide effective cooling. The estimated residence time of the TD was ~1.9 seconds at operated flow rate of 5 LPM. An automatic temperature-control system was also developed, of which the K type thermocouple was placed in the middle of the tubing wall to monitor the temperature. Temperature profile of actual sample air for our TD (see Fig. S2) showed good temperature accuracy and homogeneity, which has high exit temperature to avoid recondensation before evaporated gases were adsorbed by activated charcoal. TD losses are inevitable due to sedimentation, diffusion and thermophoresis inside the heating tube. In this work, we use elemental carbon (EC) which is refractory at high temperature to quantify the temperature-dependent TD loss at different temperature (i.e., 25°C, 100°C, 150°C, 200°C, 280°C), by collecting filter samples through TD and non-TD lines with two cascade $PM_{2.5}$ impactors. EC was then measured with an OCEC analyzer (Sunset Laboratory Inc.), following the NIOSH 5040 protocol (Birch and Cary, 1996). A transmission efficiency equation as a function of temperature $\eta_t = 1.0111–0.0003 \times T$ ($R = –0.79$, $p < 0.01$, see Fig. S3) was then determined, in which η_t is transmission efficiency and T is the set temperature in Celsius (°C). All calculations below were corrected by applying this transmission efficiency. Without this correction, E_{abs} will be overestimated.

Aethalometer (AE33) and Aerosol Chemical Speciation MonitoR (ACSM)

The equivalent BC mass concentration (EBC) and light absorption coefficient were determined by filter-based AE33, which applies the dual spot technique to deal with loading effect via an internal loading correction (Drinovec *et al*., 2015). Multiple scattering effect induced from accumulated particles would interfere the signal, while it could be eliminated and nullified by using a deep mat of optically-scattering fibers as filter tape, and only the correction for multiple scattering induced by filter fiber need to be dealt with, i.e., data divided by the multiple scattering parameter, usually called C factor, C = 2.14 for quartz filter type as used in this work. Thus, data from AE33 were more guaranteed and exempted from multiple correction algorithms (Coen *et al*., 2010). Measurement of light absorption coefficient was performed using AE33 to evaluate the absorption amplification of BC by coating materials. With increasing TD temperature, the coatings on BC are expected to evaporate by different degree resulting in the change in light absorption and absorption enhancement (E_{abs}) can be also determined.

Many similar studies use photoacoustic spectrometer (PAS) to determine E_{abs}, since particles remain suspended in the air in PAS light absorption measurement, whereas particle light absorption must be measured after collection on a filter for filter-based instrument such as Aethalometer,

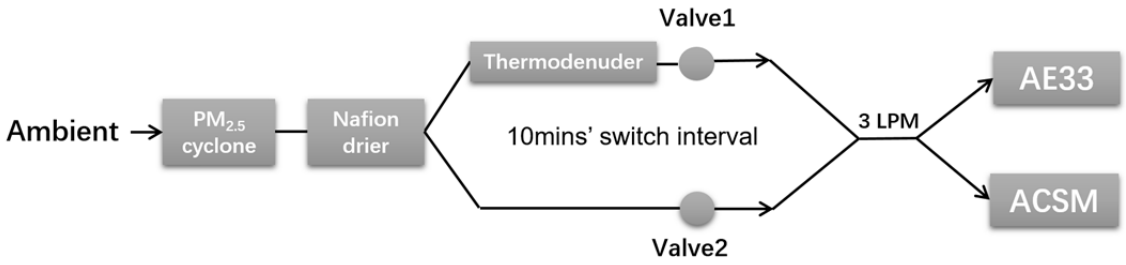

Fig. 1 System setup diagram.

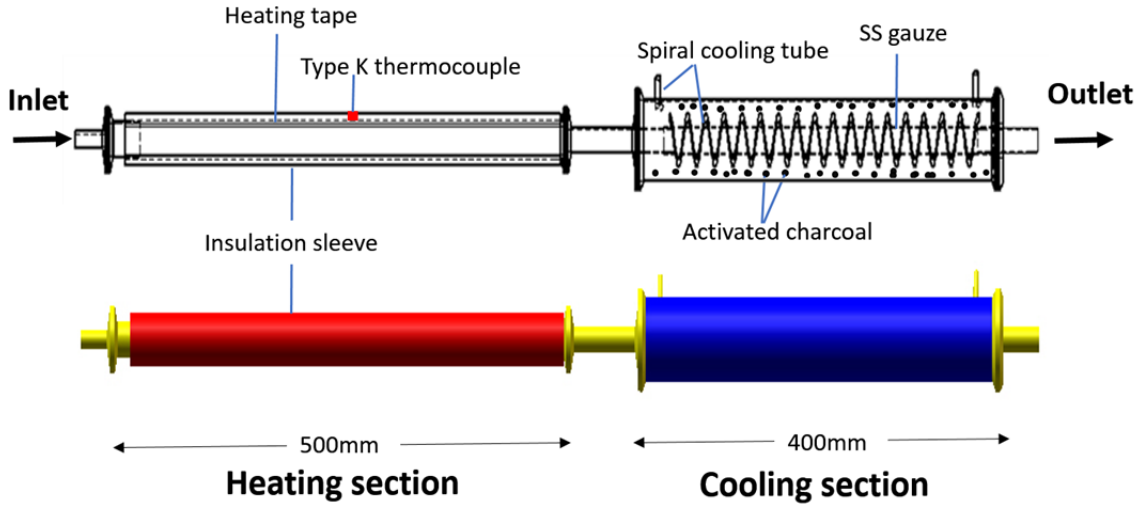

Fig. 2. Design schematic of the thermodenuder.

Particle Soot Absorption Photometer (PSAP), Multi Angle Absorption Photometer (MAAP) etc. However, filter-based instrument is more widespread in determining BC light absorption as they are inexpensive, easy to operate and can run unattended for long time despite the drawback that particle morphology won't be maintained after deposition. Moreover, light absorption variation by mixing state can also be acquired from filter-based measurement as we will discuss below. Here in order to distinguish E_{abs} evaluated from PAS, we use $E_{abs\text{-}fb}$ in this work, i.e., filter-based light absorption enhancement. And $E^{T,\lambda}_{abs-fb}$, representing $E_{abs\text{-}fb}$ calculated at different wavelength and different TD temperature, was calculated as below:

$$E^{T,\lambda}_{abs-fb} = \frac{\left[b^{\lambda}_{abs-amb}(t_{i-1}) + b^{\lambda}_{abs-amb}(t_{i+1})\right]/2}{b^{T,\lambda}_{abs-TD}(t_i)} \quad (1)$$

where $b^{T,\lambda}_{abs-TD}(t_i)$ is light absorption coefficient (b_{abs}) from sample through TD at T °C (i.e., 50°C, 100°C, 150°C, 200°C, 280°C) at wavelength of λ while at time of t_i. b_{abs} was calculated by multiplying EBC concentration from AE33 with mass absorption cross-section (MAC) from Drinovec *et al*. (2015), which has already taken into account of multiple correction. $b^{\lambda}_{abs-amb}(t_{i-1})$ and $b^{\lambda}_{abs-amb}(t_{i+1})$ represent b_{abs} at wavelength of λ corresponding to ambient measurements before and after the TD measurement, respectively, and average of the two was regarded as ambient b_{abs} without TD at time of t, in order to reduce uncertainty induced by fluctuation of time-changing aerosol concentration and composition.

Absorption Angström exponent (AAE) was determined by fitting b_{abs} to the 7 wavelengths with a power law equation (Lim *et al*., 2014), since it's likely that fitting method with seven wavelengths will give more robust value to avoid misinterpretation (Lack and Cappa, 2010).

In parallel with BC measurement by AE33, other aerosol fractions were measured by ACSM, which is built upon the same technology as Aerodyne Aerosol Mass Spectrometer (AMS). Detailed introduction to ACSM could be found in Ng *et al*. (2011). Briefly, particles with aerodynamic diameter ~40–1000 nm are sampled into ACSM through a critical orifice mounted at the inlet of an aerodynamic lens, and then are directed onto a resistively heated surface (~600°C) where particle components are flash vaporized and ionized by 70 eV electron impact. The positive ions are then analyzed by a quadruple mass spectrometer. The ACSM was calibrated for standard NO_3^- Response Factor (RF) as well as the NH_4^+ and SO_4^{2-} Relative Ionization Efficiencies (RIE), with NH_4NO_3 and $(NH_4)_2SO_4$ in sequence. The size-selected 300-nm NH_4NO_3 and $(NH_4)_2SO_4$ particles with multiple concentrations were sampled into both the ACSM and a condensation particle counter (CPC). The new RF for NO_3^- and IE for NH_4^+ and SO_4^{2-} were then determined by comparing the response factors of ACSM to the mass calculated with the known particle size and the number concentrations from CPC.

As with BC measurement, with increasing TD temperature, more semi-volatile aerosol fractions will be evaporated, as will be determined by ACSM. The remaining percentage (RP_T) of aerosol mass fractions was then quantified as below:

$$RP_{f,T} = \frac{Aerosol^{f}_{T,TD}(t_i)}{\left[Aerosol_{f,amb}(t_{i-1}) + Aerosol_{f,amb}(t_{i+1})\right]/2} \quad (2)$$

where $RP_{f,T}$ is the remaining percentage of aerosol fraction f with TD heated at T °C, $Aerosol^{f}_{T,TD}(t_i)$ is concentration of aerosol f with TD measurement at time t_i. $Aerosol_{f,amb}(t_{i-1})$ and $Aerosol_{f,amb}(t_{i+1})$ is concentration of ambient aerosol f before and after TD measurement.

Core-Shell Mie Model Calculation

Mie calculation was performed using the same MATLAB code as in Mätzler (2002a, b), who wrote the program according to Bohren and Huffman (1983). As for input parameters, refractive index (RI) of BC and BC coating at

certain wavelength, size of BC core and shell, and particle density are needed to calculate the absorption cross section σ_{abs}^{λ}.

Input size for BC core was constrained based on our previous study (Ning *et al*., 2013), which measured the BC mass size distribution of diesel engine exhaust by tandem of DMA, Aethalometer and CPC (DMA-Aeth-CPC). Mass size distribution was then converted to BC-containing particles number size distribution (see Fig. S4), assuming the density of BC is 1.8 g cm^{-3} as recommended by Bond *et al*. (2006). Geometric mean diameter (GMD) was adopt regarding size parameter in Mie. GMD and Geometric standard deviation (GSD) of BC mass size distribution was then determined with following equation:

$$MD = \exp\left(\frac{\sum_l^u n \cdot \ln D_p}{N}\right) \quad (3)$$

$$SD = \exp\left(\sqrt{\frac{\sum_l^u n\left(\ln D_p - \ln GMD\right)^2}{N}}\right) \quad (4)$$

where l is lower size, u is upper size, n is BC-containing particle number concentration at certain size, N is total number concentration of BC. D_p is corresponding particle diameter.

Calculated GMD and GSD was 70 nm and 1.7, respectively, which was regarded as BC core diameter ($D_{p,\,core}$) and will be then fit to a lognormal size distribution. The size of BC shell and refractive index for BC core and coating will be discussed in following section.

RESULTS AND DISCUSSION

Characterization of Ambient Aerosol

Figs. 3(a) and 3(b) shows the hourly averaged mass concentration for five non-refractory PM_1 (NR-PM_1) species and equivalent BC (EBC) at seven wavelengths during the experiment period. Total NR-PM_1 concentrations varied from 2.7 to 51.7 μg m^{-3} (see also Table 1), with an average of 25.3 ± 9.8 μg m^{-3}. Organics (Org) and sulfate (SO_4^{2-}) were two dominant species, with relative contribution of 51.3% and 29.0% to NR-PM_1, followed by ammonium (NH_4^+, 11.2%), nitrate (NO_3^-, 8.0%) and chloride (Chl, 0.4%), which is similar to other studies in Hong Kong (Sun *et al*., 2016) and in Beijing (Sun *et al*., 2013). PMF analysis on organic aerosol (OA) (see Fig. S5) showed that oxygenated OA (OOA) accounted for 55% of all organic aerosol, followed by hydrocarbon-like OA (HOA), accounting for 45%. As can be seen in Fig. 3(b), EBC at 370 nm (BC370), also called UV-absorbing particulate material (UVPM), always showed higher concentration than EBC at long wavelengths such as BC880, usually regarded as BC, indicating the presence of additional UV-specific absorbing compounds. As is also indicated by correlation analysis between organics and seven wavelengths EBC, i.e., correlation coefficient (R ≈ 0.75, $p < 0.01$) was slightly higher between organics and EBC in short wavelengths.

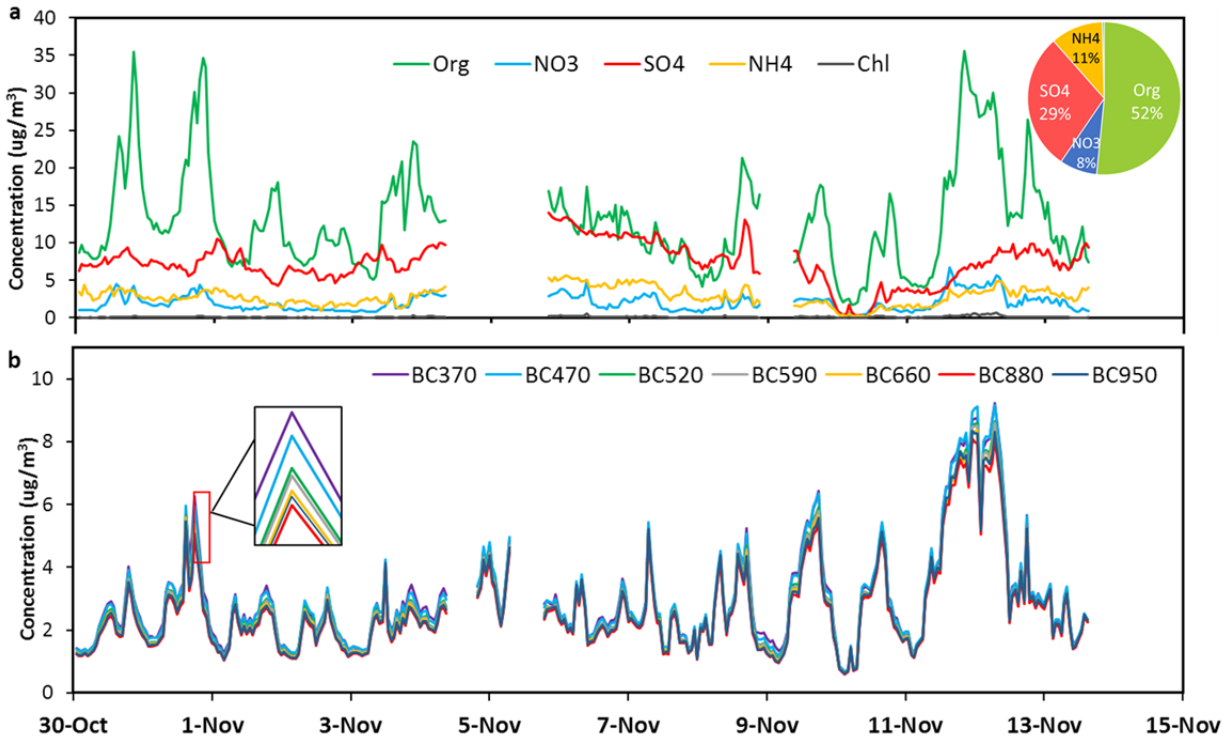

Fig. 3. Temporal variation of mass concentration for (a) non-refractory PM_1 species (organics (Org), nitrate (NO_3), sulfate (SO_4), ammonium (NH_4) and chloride (Chl)); (b) equivalent BC (EBC) at seven wavelengths (370 nm, 470 nm, 520 nm, 590 nm, 660 nm, 880 nm, 950 nm).

Table 1. Statistics description and correlation coefficient for NRPM1 species and EBC.

Species	Statistics				Pearson Correlation (R value)			
	Min	Max	Average	Std	Org	NO_3	SO_4	NH_4
Org	1.8	35.6	13.0	6.7	1.0	0.78**	0.35**	0.46**
NO_3	0.2	6.7	2.0	1.2	0.78**	1.0	0.40**	0.60**
SO_4	0.2	14.0	7.3	2.2	0.35**	0.40**	1.0	0.94**
NH_4	0.1	5.7	2.8	2.2	0.46**	0.60**	0.94**	1.0
Chl	0.1	0.7	0.1	0.1	0.65**	0.75**	0.14*	0.32**
NRPM1	2.7	51.7	25.3	9.8	0.91**	0.84**	0.69**	0.78**
BC370	0.6	9.2	3.0	1.7	0.75**	0.72**	0.03	0.19**
BC470	0.7	9.2	3.0	1.7	0.74**	0.72**	0.03	0.19**
BC520	0.6	8.7	2.8	1.6	0.73**	0.72**	0.04	0.20**
BC590	0.6	8.6	2.8	1.6	0.73**	0.72**	0.04	0.20**
BC660	0.6	8.4	2.7	1.6	0.73**	0.72**	0.04	0.20**
BC880	0.6	8.1	2.6	1.5	0.73**	0.73**	0.04	0.21**
BC950	0.6	8.3	2.7	1.6	0.72**	0.72**	0.04	0.21**

** Correlation is significant at the 0.01 level (2-tailed).

* Correlation is significant at the 0.05 level (2-tailed).

Significant correlation relationship between nitrate, organics and EBC was also observed, indicating similar sources possibly typical urban vehicular emission. Absorption Angström exponent (AAE) of 1.05–1.17 (Fig. 5) was observed for ambient aerosol (i.e., before heating), similar to AAE of 1.1 for aerosol from traffic source reported by Sandradewi *et al*. (2008), suggesting main source of BC probably from traffic rather than others such as biomass burning, which would have a larger AAE due to the presence of brown carbon (BrC) (Russell *et al*., 2010). As is also indicated from BC source apportionment by AE33 based on model in Sandradewi *et al*. (2008), 89.2 ± 3% was apportioned to fossil fuel combustion (i.e., traffic emission), followed by biomass burning 10.8 ± 3%. Correlation relationship between sulfate or ammonium and EBC was weak, but sulfate and ammonium was strongly correlated, which is justifiable since ammonium sulfate were usually present in the same particle mode (Takami *et al*., 2005). Ratio of ammonium to sulfate is about 0.87, similar to other studies (Hatakeyama *et al*., 2004; Takami *et al*., 2005), indicating slightly acidic aerosol. With regards to chloride, measured concentration was too low, so we don't discuss it here.

Characterization of Heated Aerosol

We evaluated the filter-based light absorption enhancement of BC ($E_{abs-fb}^{T,\lambda}$) as well as the remaining aerosol compositions indicated by remaining percentage (*RP*) for aerosol passing through TD at certain temperature.

As shown in Fig. 4(a), all NR-PM_1 species decreased with increase of TD heating temperature, but decreasing pattern varied from each other, which was probably attributed to different mechanisms of these fractions such as evaporation and chemical dissociation. Organics with *RP* of ~30% after heating at 200°C, even at 280°C, there were still 23% of low-volatility organics left (3.2 ± 0.8 μg m^{-3}), indicating the wide range of volatility for organic aerosol. For nitrate, heating at 150°C resulted in an *RP* of ~35% (1.0 ± 0.4 μg m^{-3}), similar to observation reported by Bi *et al*. (Bi *et al*., 2015). *RP* of 13% (0.5 ± 0.1 μg m^{-3}) for nitrate was still observed at 280°C, which may due to little recondensation. Sulfate was observed to be refractory below 200°C, with only 20% drop of *RP*. While heated up to 280°C, a sharp decrease of sulfate *RP* was detected with *RP* of 36% (3.5 ± 0.6 μg m^{-3}), showing low volatility of sulfate which is similar to that found in Bi *et al*. (2015) and Zhai *et al*. (2015). Regarding ammonium, it was notable that, the decrement of RP for ammonium from 50 to 100°C (21%), 100 to 150°C (23%) and 150 to 200°C (9%) was significantly correlated to that of nitrate (0.99, $p < 0.01$), i.e., 19%, 19% and 12% respectively, indicating that these were likely constituent NH_4NO_3, thus ammonium was volatilized along with nitrate. NH_4NO_3 almost vanished at 200°C. Then from 200 to 280°C, we observed a rapid decrease of ammonium and sulfate, with a similar decrement of RP of 49% and 43%, respectively, suggesting the bond of NH_4^+ and SO_4^{2-}, and/or conjunction of HSO_4^- and NH_4^+ (Zhai *et al*., 2015).

Parallel light absorption measurement by AE33 (see Fig. 4(b)) showed that, with heating temperature from 50°C to 200°C, E_{abs-fb} generally showed a slight increase from 1.02 ($E_{abs-fb}^{50°C,880}$) to 1.20 ($E_{abs-fb}^{200°C,660}$). While as TD was heated at 280°C, E_{abs-fb} increased sharply to ~1.64 ($E_{abs-fb}^{280°C,660}$), implying a significant light absorption amplification due to the mixing with other aerosol fractions, which were together collected onto the filter tape where light attenuation was then measured. As discussed above, *RP* of organics and nitrate decreased very little from 200°C to 280°C, whereas sulfate and ammonium showed a remarkable decrease, indicating a significant impact of ammonium sulfate on light absorption enhancement, due to their lensing effect by coatings. Compared to other studies of E_{abs} by field observation using TD, as summarized in Table 2, E_{abs} would vary to large extent depending on the location, source, sampling period and TD heating temperature.

In addition, Lack *et al*. (2008) and Cappa *et al*. (2008) reported a significantly positive bias of absorption by filter-based light absorption measurement using PSAP, and

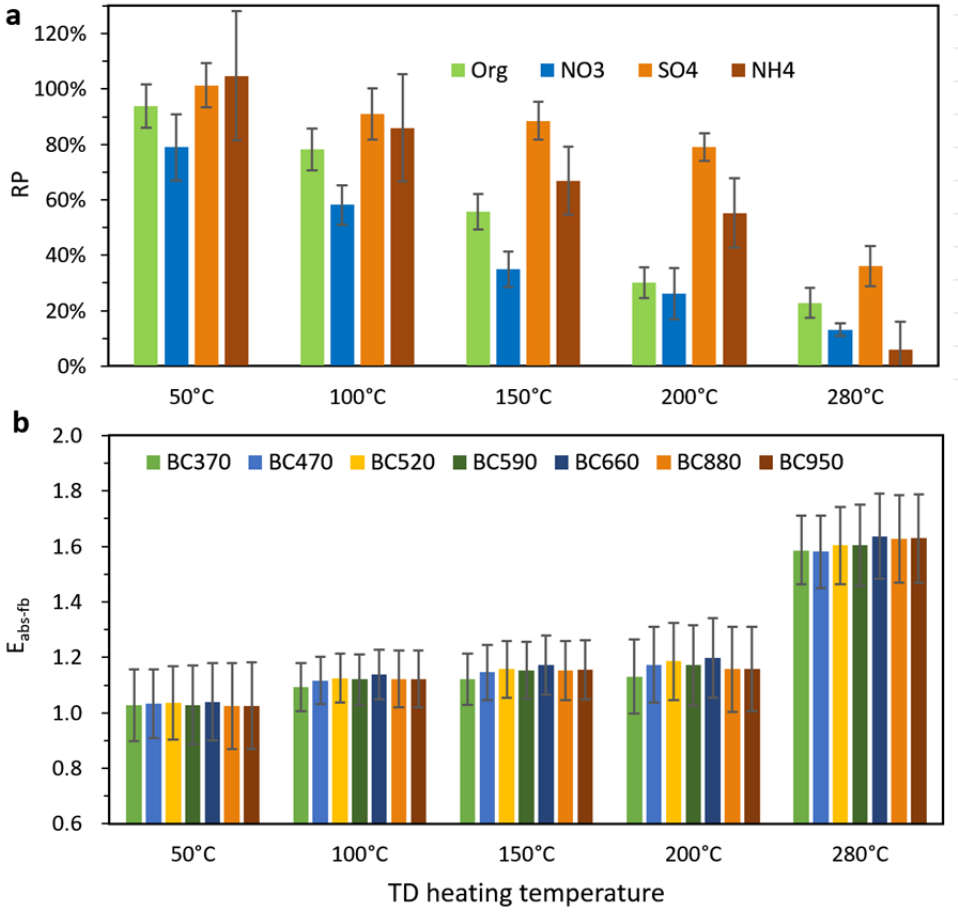

Fig. 4. (a) Remaining percentage (*RP*) of four aerosol fractions (i.e., organics, nitrate, sulfate and ammonium), and (b) $E_{abs\text{-}fb}$ at seven wavelengths under different TD heating temperature; Error bar represent the standard error (SE).

speculated that such biases might be due to the redistribution of liquid-like organic aerosols (OA) around filter. Consequently, possible artificial coating by OA might induce light absorption enhancement of BC. However, according to our observation, organics don't have notable impact on E_{abs}, since organics varied little for heated aerosol from 200 to 280°C, whereas $E_{abs\text{-}fb}$ increased sharply from 1.16 ($E_{abs-fb}^{200°C,880}$) to 1.63 ($dE_{abs-fb}^{280°C,880}$). Moreover, OA was usually recognized to have stronger absorption at short wavelength, so it's reasonable to observe a positive bias at short wavelength. Therefore, it's hard to claim OA has such impact on light absorption enhancement at long wavelength here determined from Aethalometer measurement. Nevertheless, further work is needed to quantify the filter-based light absorption impact due to mixing state (in addition to OA) suspended and/or collected on filters.

Furthermore, we calculated AAE for heated aerosol passing through TD. As shown in Fig. 5, no major change but a slight increase was observed after heating with TD, implying that BrC does not significantly contribute to light absorption if internal mixing of BC does not alter AAE (Lack and Langridge, 2013). Similarly, Devi *et al.* (2016) observed an average AAE of 0.99 before heating at 200°C and 0.98 after heating at rural Centerville. Although AAE for pure uncoated BC is approximately 1, it's reasonable to observe no decrease for AAE of heated aerosol, based upon these two facts: 1) that uncoated BC has an AAE of about 1 applies to BC particles < 50 nm in diameter, it can range from 0.7–1.2 for diameters of particles > 50 nm (Gyawali *et al.*, 2009). 2) According our observation, there was still certain non-BC fraction left after heating at 280°C, whose effects on AAE were unknown. The resultant AAE discrepancy may probably be attributed to aerosol chemical composition, size and coatings, all of which could be source-specific (Lack and Langridge, 2013). Based on above discussion, in the calculation of light absorption enhancement, light absorption of BrC will not be considered.

Theoretical Calculation from Mie Model

Light absorption amplification determined by Mie theory has been found to be in good agreement with that from field observation and lab experiment (Liu *et al.*, 2015; Schnaiter *et al.*, 2005). In this work, we assumed our field measurement E_{abs} (i.e., ~1.5 to ~1.7) was well reproduced by Mie theory, and then performed inverse calculation to evaluate the coating fraction or other parameter, based on following input parameters.

BC core diameter (D_{core}) was calculated to be 70 nm as discussed above (Section 2.3.1). However, due to the

Table 2. Comparison of field observation E_{abs} reported in the literature, note that Eabs at UV wavelength (i.e., 370 nm, 404 nm and 405 nm) includes enhancement induced by semi-volatile BrC.

Location	Sampling period	TD temperature	Optical Instrument	E_{abs}(wavelength/nm)	Reference
California, USA	June	225°C	UCD-PAS	1.13 (405); 1.06 (532)	(Cappa *et al.*, 2012)
Nagoya[U], Japan	Aug.	300°C	PAS	~1.10 (781)	(Nakayama *et al.*, 2014)
Nagoya[U], Japan	Jan.	400°C	PAS	ND (781); ~1.17 (405)	(Nakayama *et al.*, 2014)
Colorado, USA	Biomass burning event	200°C	PAS	1.7–3.5 (404); 1.4 (532)	(Lack and Schwarz, 2012)
Detling[R], UK	Winter	250°C	PAS	1.3 (405); 1.4 (781)	(Liu *et al.*, 2015)
Fresno, CA, USA	Winter	275°C	PAS	1.27 ± 0.17 (405)	(Zhang *et al.*, 2016)
				1.18 ± 0.06 (532)	
				1.21 ± 0.09 (870)	
Atlanta[U], GA, USA	May	200°C	Aethalometer	~1.54 (370); ~1.25 (880)	(Devi *et al.*, 2016)
Centreville[R], AL, USA	June-July	200°C	Aethalometer	~1.25 (370 and 880)	(Devi *et al.*, 2016)
Yuen Long[U], Hong Kong	Nov.	200°C	Aethalometer (AE33)	1.13 (370); 1.16 (880)	Our study
Yuen Long[U], Hong Kong	Nov.	280°C	Aethalometer (AE33)	1.59 (370); 1.63 (880)	Our study

[U] Urban area; [R] Rural area; ND: not detected.

limitation in determining BC shell diameter (D_{shell}), i.e., not all particles in the ambient contain BC whereas mobility-based instrument such as SMPS measured the ensemble of particles. Input D_{shell} was constrained to a recommended range from 77 to 350 nm given by Bond *et al*. (2006), with coating thickness to BC core ratio of 0.1–4.0, which was quantified as $(D_{shell} - D_{core})/D_{core}$. Because there are ~20% low-volatile aerosol fractions evaporate from the particle after heating with TD at 280°C according to our observation, we assumed the same coating materials remained. $E_{abs\text{-}Mie}$ was thus determined based on Mie calculation using equation below:

$$E^{\lambda}_{abs-Mie} = \frac{\sigma^{\lambda}_{abs-core-shell}}{\sigma^{\lambda}_{abs-20\%Rcoat}} \quad (5)$$

where $\sigma^{\lambda}_{abs-core-shell}$ is normalized absorption cross section (σ^{λ}_{abs}) for an ensemble of BC-containing particles with the same coating thickness to core ratio (*Rcoat*). $\sigma^{\lambda}_{abs-20\%Rcoat}$ is normalized σ^{λ}_{abs} of BC-containing particles with only 20% × *Rcoat* of coating left.

To be consistent with AE33 for data comparison, refractive indices at the same seven wavelengths (i.e., 370, 470, 520, 590, 660, 880 and 950 nm) were selected. A fixed RI for pure BC core of 1.85–0.71*i* was applied to wavelength from 370 nm to 950 nm, following Bond *et al*. (2006). Since we don't consider the absorbing coatings such as BrC, RI of $1.5 + 10^{-6}i$ was applied to the coating part based on Lack and Cappa (2010). Result was shown in Fig. 6, with increasing *coating thickness-core ratio* from 0.5 to 4.0, $E_{abs\text{-}Mie}$ increased from 1.3 to as high as ~2.8 (370 nm). To achieve our field observed E_{abs} (~1.5 to ~1.7), the targeted *coating thickness-core ratio* should be mainly from 1.0 to 2.0 as shown by green zone.

Limitations and Perspectives

Result of this study could provide useful information for relevant studies such as climate modelling, and further our understanding on BC mixing state, while it is worth noting the inherent limitations of the findings. First, filter-based measurement for BC light absorption cannot avoid the change of certain particle morphology or mixing state, due to the accumulation of aerosol particles on filter medium. The morphology for BC-containing particles, e.g., the location of BC core in the center or edge, may influence lensing effect (Liu *et al*., 2015). While it seems impossible to consider the morphology in the accumulated particles on the filter, what we conclude in this work was more likely a statistic or microscopic result reflected by all aerosol particles collected on the filter. Second, the multiple scattering parameter C factor (i.e., 2.14) could be enhanced if very high concentrations of semi-volatile gaseous species absorbed onto the filter (Weingartner *et al*., 2003), thus care should be taken when treating the enhancement negligible for ambient measurement. There are also limitations with the application of Mie model. Many studies often applied

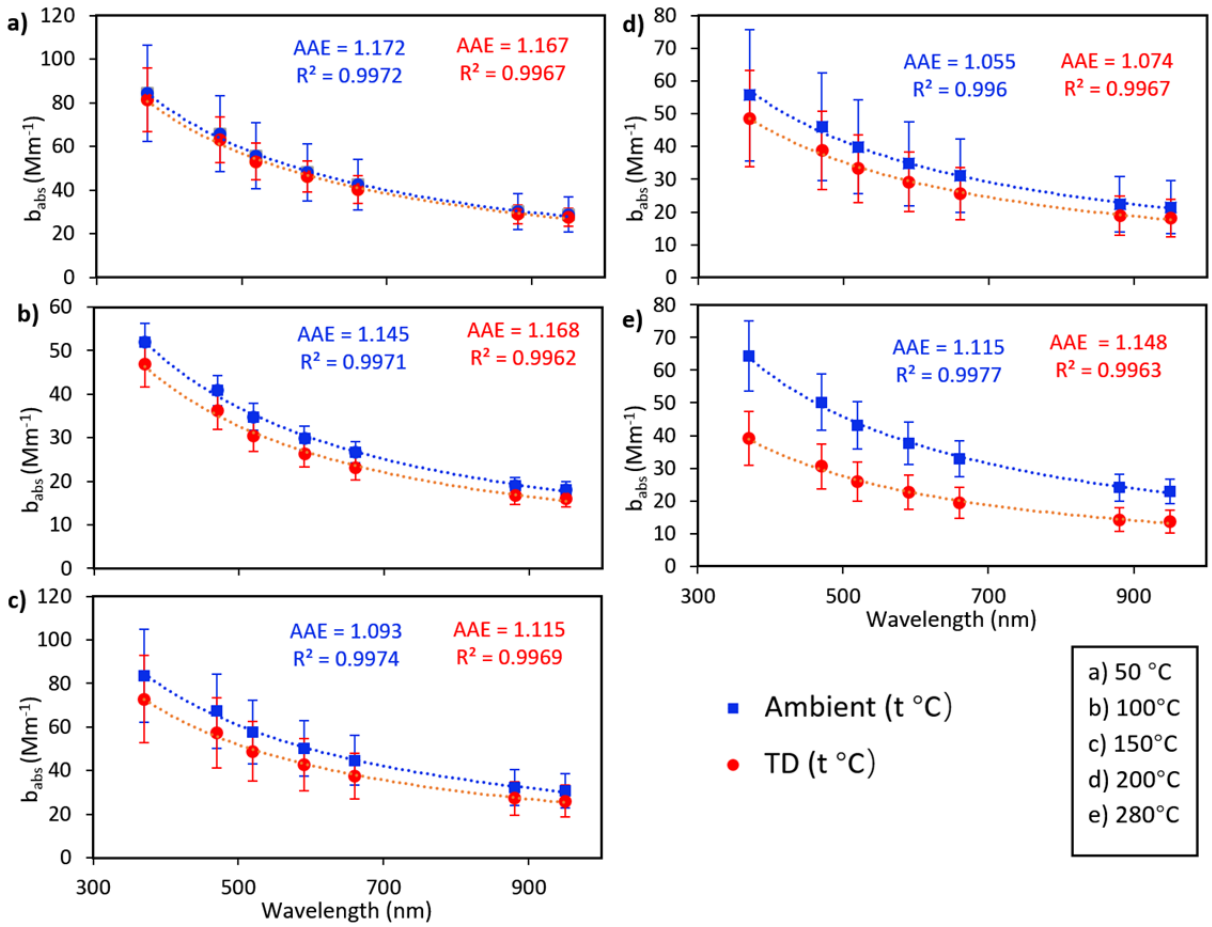

Fig. 5. Light absorption coefficient (b_{abs}) and fitted AAE of heated (T temperature) and corresponding ambient aerosol.

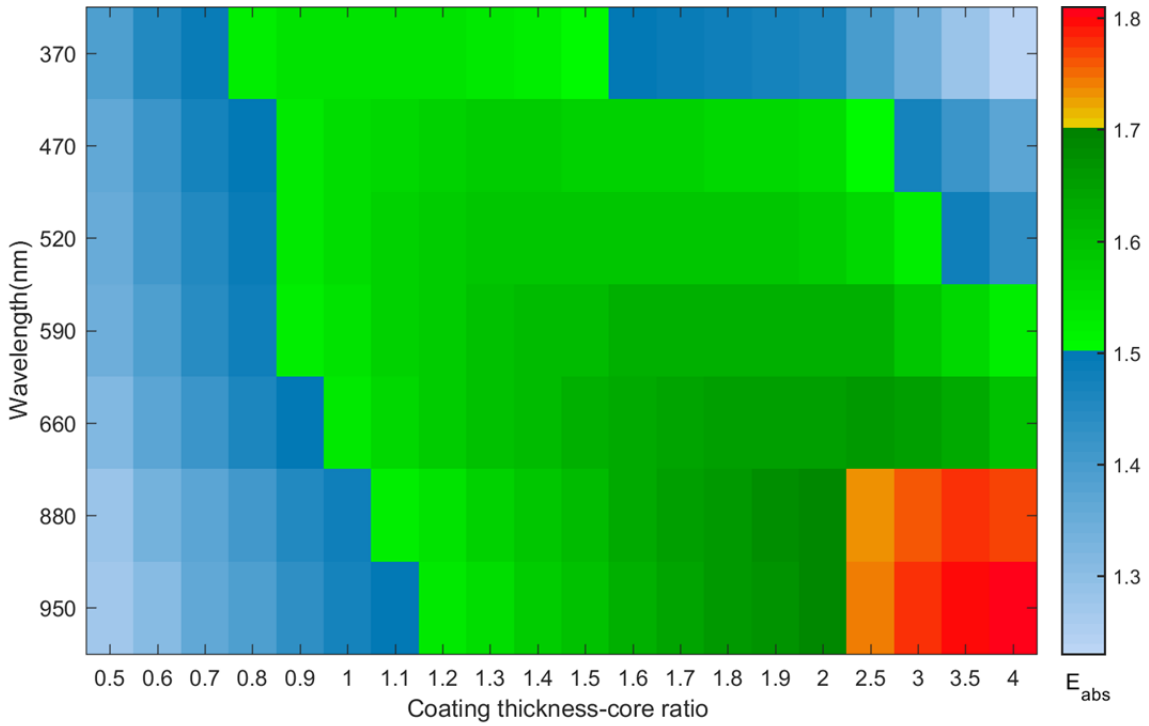

Fig. 6. Assuming 20% coatings remained, a) E_{abs} calculated by Mie theory based on different coating fraction. Green zone was targeted area for Mie calculation in well agreement with field measurement.

different parameter values (Bond *et al*., 2006; Lack and Cappa, 2010; Cappa *et al*., 2012; Liu *et al*., 2015). Mie theory assumes the shape of particles is spherical, and coated evenly on BC core, whereas BC core is observed to be irregularly chain-like shaped, and coating might not be fully coated onto BC core (Bond and Bergstrom, 2006; Liu *et al*., 2016). It's not simple to directly measure the mixing state, which must be achieved by single-particle methods or microscopy. Moreover, particles are unlikely well mixed in the atmosphere, and simulations are key to estimating their average climate effect (Bond *et al*., 2006). And there are also several different modelling methods other than Mie theory such as Rayleigh-Debye-Gans (RDG) approximation, discrete dipole approximation (DDA) etc. (Liu *et al*., 2015; Liu *et al*., 2016). Besides, future investigations on aerosols from different sources and environment conditions are needed to verify the heterogeneity of BC mixing state and its impact to light absorption. Besides, longer period observation should also be performed to capture the diurnal profile of E_{abs}, since the mixing state may change quickly in different hours each day.

CONCLUSION

In this work, field observations of aerosol absorption were conducted in Hong Kong. A homemade thermodenuder (TD) was then applied to remove the semi-volatile fraction at graduated temperatures between 50 and 280°C. Afterward, an ACSM was used to characterize the remaining chemical species of the non-refractory PM_1, and an advanced aethalometer was used to measure the remaining black carbon (BC) and the light absorption coefficient (b_{abs}). Results show that as the heating temperature increased, more semi-volatile species evaporated, e.g., nitrate and organics were vaporized from 150 to 200°C, although ammonium and sulfate showed a low volatility, evaporating at temperatures below 280°C. Measurements of the parallel light absorption showed that E_{abs} varied little, from 1.02 to 1.20, at TD heating temperatures between 50 and 200°C but skyrocketed to ~1.6 at 280°C, indicating the lensing effect by ammonium sulfate on the enhancement of light absorption. The absorption Angström exponent (AAE) was around 1.1–1.2, with negligible change after heating, implying that BrC does not significantly contribute to light absorption. Mie model calculations were performed to inversely determine the coating fraction. Results show that the coating fraction is about 100–200%. Although this study provides much information for relevant studies, such as climate modelling, due to the limitation of filter-based instruments, further studies, such as a combination or comparison of different methods, should be conducted to verify and evaluate the effectiveness of coatings.

ACKNOWLEDGEMENT

The work described in this paper was partial supported by the grant from the Research Grants Council of the Hong Kong Special Administrative Region, China (RGC Project No.11204115 and No. 21201214). The authors would also like to thank the support from Guy Carpenter Asia-Pacific Climate Impact Centre at City University of Hong Kong (Project No. 9667102).

SUPPLEMENTARY MATERIAL

Supplementary data associated with this article can be found in the online version at http://www.aaqr.org.

REFERENCE

Bi, X., Dai, S., Zhang, G., Qiu, N., Li, M., Wang, X., Chen, D., Peng, P., Sheng, G., Fu, J. and Zhou, Z. (2015). Real-time and single-particle volatility of elemental carbon-containing particles in the urban area of Pearl River Delta region, China. *Atmos. Environ.* 118: 194–202.

Birch, M.E. and Cary RA (1996). Elemental carbon-based method for monitoring occupational exposures to particulate diesel exhaust. *Aerosol Sci. Technol.* 25: 221–241.

Bohren, C.F. and Huffman, D.R. (1983). *Absorption and scattering of light by small particles*. John Wiley & Sons.

Bond, T.C. and Bergstrom, R.W. (2006). Light absorption by carbonaceous particles: An investigative review. *Aerosol Sci. Technol.* 40: 27–67.

Bond, T.C., Habib, G. and Bergstrom, R.W. (2006). Limitations in the enhancement of visible light absorption due to mixing state. *J. Geophys. Res.* 111: D20.

Bond, T.C., Doherty, S.J., Fahey, D.W., Forster, P.M., Berntsen, T., DeAngelo, B.J., Flanner, M.G., Ghan, S., Kärcher, B., Koch, D., Kinne, S., Kondo, Y., Quinn, P.K., Sarofim, M.C., Schultz, M.G., Schulz, M., Venkataraman, C., Zhang, H., Zhang, S., Bellouin, N., Guttikunda, S.K., Hopke, P.K., Jacobson, M.Z., Kaiser, J.W., Klimont, Z., Lohmann, U., Schwarz, J.P., Shindell, D., Storelvmo, T., Warren, S.G. and Zender, C.S. (2013). Bounding the role of black carbon in the climate system: A scientific assessment. *J. Geophys. Res.* 118: 5380–5552.

Burtscher, H., Baltensperger, U., Bukowiecki, N., Cohn, P., Hüglin, C., Mohr, M., Matter, U., Nyeki, S., Schmatloch, V., Streit, N. and Weingartner, E. (2001). Separation of volatile and non-volatile aerosol fractions by thermodesorption: Instrumental development and applications. *J. Aerosol Sci.* 32: 427–442.

Cappa, C.D., Lack, D.A., Burkholder, J.B. and Ravishankara, A.R. (2008). Bias in filter-based aerosol light absorption measurements due to organic aerosol loading: Evidence from laboratory measurements. *Aerosol Sci. Technol.* 42: 1022–1032.

Cappa, C.D., Onasch, T.B., Massoli, P., Worsnop, D.R., Bates, T.S., Cross, E.S., Davidovits, P., Hakala, J., Hayden, K.L., Jobson, B.T., Kolesar, K.R., Lack, D.A., Lerner, B.M., Li, S.M., Mellon, D., Nuaaman, I., Olfert, J.S., Petäjä, T., Quinn, P.K., Song, C., Subramanian, R., Williams, E.J. and Zaveri, R.A. (2012). Radiative absorption enhancements due to the mixing state of atmospheric black carbon. *Science* 337: 1078–1081.

Cheng, Y., Lin, C., Liu, J. and Hsieh, C. (2014). Temporal characteristics of black carbon concentrations and its potential emission sources in a southern Taiwan industrial urban area. *Environ. Sci. Pollut. Res.* 21: 3744–3755.

Collaud Coen, M., Weingartner, E., Apituley, A., Ceburnis, D., Fierz-Schmidhauser, R., Flentje, H., Henzing, J.S., Jennings, S.G., Moerman, M., Petzold, A., Schmid, O. and Baltensperger, U. (2010). Minimizing light absorption measurement artifacts of the Aethalometer: Evaluation of five correction algorithms. *Atmos. Meas. Tech.* 3: 457–474.

Devi, J.J., Bergin, M.H., Mckenzie, M., Schauer, J.J. and Weber, R.J. (2016). Contribution of particulate brown carbon to light absorption in the rural and urban Southeast US. *Atmos. Environ.* 136: 95–104.

Drinovec, L., Močnik, G., Zotter, P., Prévôt, A.S.H., Ruckstuhl, C., Coz, E., Rupakheti, M., Sciare, J., Müller, T., Wiedensohler, A. and Hansen, A.D.A. (2015). The "dual-spot" Aethalometer: An improved measurement of aerosol black carbon with real-time loading compensation. *Atmos. Meas. Tech.* 8: 1965–1979.

Fuller, K.A., Malm, W.C. and Kreidenweis, S.M. (1999). Effects of mixing on extinction by carbonaceous particles. *J. Geophys. Res.* 104: 15941–15954.

Gyawali, M., Arnott, W.P., Lewis, K. and Moosmüller, H. (2009). In situ aerosol optics in Reno, NV, USA during and after the summer 2008 California wildfires and the influence of absorbing and non-absorbing organic coatings on spectral light absorption. *Atmos. Chem. Phys.* 9: 8007–8015.

Hatakeyama, S., Takami, A., Sakamaki, F., Mukai, H., Sugimoto, N., Shimizu, A. and Bandow, H. (2004). Aerial measurement of air pollutants and aerosols during 20-22 March 2001 over the East China Sea. *J. Geophys. Res.* 109: D13304.

IPCC (2007). *Climate Change 2007: The Physical Science Basis*. Contribution of Working Group I to the Fourth Assessment, Cambridge University Press, Cambridge, United Kingdom, and New York, NY, USA.

Jacobson, M.Z. (2001). Strong radiative heating due to the mixing state of black carbon in atmospheric aerosols. *Nature* 409: 695–697.

Lack, D.A., Cappa, C.D., Covert, D.S., Baynard, T., Massoli, P., Sierau, B., Bates, T.S., Quinn, P.K., Lovejoy, E.R. and Ravishankara, A.R. (2008). Bias in filter-based aerosol light absorption measurements due to organic aerosol loading: Evidence from ambient measurements. *Aerosol Sci. Technol.* 42: 1033–1041.

Lack, D.A. and Cappa, C.D. (2010). Impact of brown and clear carbon on light absorption enhancement, single scatter albedo and absorption wavelength dependence of black carbon. *Atmos. Chem. Phys.* 10: 4207–4220.

Lack, D.A. and Schwarz, J.P. (2012). Brown carbon and internal mixing in biomass burning particles. *Proc. Natl. Acad. Sci. U.S.A.* 109: 14802–14807.

Lack, D.A. and Langridge, J.M. (2013). On the attribution of black and brown carbon light absorption using the Ångström exponent. *Atmos. Chem. Phys. Discuss*. 13: 15493–15515.

Lim, S., Lee, M., Kim, S.W., Yoon, S.C., Lee, G. and Lee, Y.J. (2014). Absorption and scattering properties of organic carbon versus sulfate dominant aerosols at Gosan climate observatory in Northeast Asia. *Atmos. Chem. Phys.* 14: 7781–7793.

Liu, F., Yon, J. and Bescond, A. (2016). On the radiative properties of soot aggregates – Part 2: Effects of coating. *J. Quant. Spectrosc. Radiat.* 172: 134–145.

Liu, S., Aiken, A.C., Gorkowski, K., Dubey, M.K., Cappa, C.D., Williams, L.R., Herndon, S.C., Massoli, P., Fortner, E.C., Chhabra, P.S., Brooks, W.A., Onasch, T.B., Jayne, J.T., Worsnop, D.R., China, S., Sharma, N., Mazzoleni, C., Xu, L., Ng, N.L., Liu, D., Allan, J.D., Lee, J.D., Fleming, Z.L., Mohr, C., Zotter, P., Szidat, S. and Prévôt, A.S.H. (2015). Enhanced light absorption by mixed source black and brown carbon particles in UK winter. *Nat. Commun.* 6: 8435.

Mätzler C (2002b). *MATLAB functions for Mie scattering and absorption, version 2*. Institute of Applied Physics, Research Report, pp. 1–24.

Mätzler, C. (2002a). *MATLAB functions for Mie scattering and absorption*. Institute of Applied Physics, Research Report, pp. 1–16.

Moffet, R.C. and Prather, K.A. (2009). In-situ measurements of the mixing state and optical properties of soot with implications for radiative forcing estimates. *Proc. Natl. Acad. Sci. U.S.A.* 106: 11872–11877.

Nakayama, T., Ikeda, Y., Sawada, Y., Setoguchi, Y., Ogawa, S., Kawana, K., Mochida, M., Ikemori, F., Matsumoto, K. and Matsumi, Y. (2014). Properties of light-absorbing aerosols in the Nagoya urban area, Japan, in August 2011 and January 2012: Contributions of brown carbon and lensing effect. *J. Geophys. Res.* 119: 12721–12739.

Ng, N.L., Herndon, S.C., Trimborn, A., Canagaratna, M.R., Croteau, P.L., Onasch, T.B., Sueper, D., Worsnop, D.R., Zhang, Q., Sun, Y.L. and Jayne, J.T. (2011). An Aerosol Chemical Speciation Monitor (ACSM) for routine monitoring of the composition and mass concentrations of ambient aerosol. *Aerosol Sci. Technol.* 45: 780–794.

Ning, Z., Chan, K.L., Wong, K.C., Westerdahl, D., Močnik, G., Zhou, J.H. and Cheung, C.S. (2013). Black carbon mass size distributions of diesel exhaust and urban aerosols measured using differential mobility analyzer in tandem with Aethalometer. *Atmos. Environ.* 80: 31–40.

Ramanathan, V. and Carmichael, G. (2008). Global and regional climate changes due to black carbon. *Nat. Geosci.* 1: 221–227.

Russell, P.B., Bergstrom, R.W., Shinozuka, Y., Clarke, A.D., DeCarlo, P.F., Jimenez, J.L., Livingston, J.M., Redemann, J., Dubovik, O. and Strawa, A. (2010). Absorption Angstrom Exponent in AERONET and related data as an indicator of aerosol composition. *Atmos. Chem. Phys.* 10: 1155–1169.

Sandradewi, J., Prévôt, A.S.H., Szidat, S., Perron, N., Alfarra, M.R., Lanz, V.A., Weingartner, E. and Baltensperger, U. (2008). Using aerosol light absorption measurements for the quantitative determination of wood burning and traffic emission contributions to particulate matter. *Environ.*

Sci. Technol. 42: 3316–3323.

Schnaiter, M., Linke, C., Möhler, O., Naumann, K.H., Saathoff, H., Wagner, R., Schurath, U. and Wehner, B. (2005). Absorption amplification of black carbon internally mixed with secondary organic aerosol. *J. Geophys. Res.* 110: D19204.

Shiraiwa, M., Kondo, Y., Iwamoto, T. and Kita, K. (2010). Amplification of light absorption of black carbon by organic coating. *Aerosol Sci. Technol.* 44: 46–54.

Srivastava, A.K., Singh, S., Tiwari, S. and Bisht, D.S. (2012). Contribution of anthropogenic aerosols in direct radiative forcing and atmospheric heating rate over Delhi in the Indo-Gangetic Basin. *Environ. Sci. Pollut. Res.* 19: 1144–1158.

Sun, C., Lee, B.P., Huang, D., Jie Li, Y., Schurman, M.I., Louie, P.K.K., Luk, C. and Chan, C.K. (2016). Continuous measurements at the urban roadside in an Asian megacity by Aerosol Chemical Speciation Monitor (ACSM): particulate matter characteristics during fall and winter seasons in Hong Kong. *Atmos. Chem. Phys.* 16: 1713–1728.

Sun, Y.L., Wang, Z.F., Fu, P.Q., Yang, T., Jiang, Q., Dong, H.B., Li, J. and Jia, J.J. (2013). Aerosol composition, sources and processes during wintertime in Beijing, China. *Atmos. Chem. Phys.* 13: 4577–4592.

Takami, A., Miyoshi, T., Shimono, A. and Hatakeyama, S. (2005). Chemical composition of fine aerosol measured by AMS at Fukue Island, Japan during APEX period. *Atmos. Environ.* 39: 4913–4924.

Wehner, B., Philippin, S. and Wiedensohler, A. (2002). Design and calibration of a thermodenuder with an improved heating unit to measure the size-dependent volatile fraction of aerosol particles. *J. Aerosol Sci.* 33: 1087–1093.

Weingartner, E., Saathoff, H., Schnaiter, M., Streit, N., Bitnar, B. and Baltensperger, U. (2003), Absorption of light by soot particles: Determination of the absorption coefficient by means of aethalometers. *J. Aerosol Sci.* 34: 1445–1463.

You, R., Radney, J.G., Zachariah, M.R. and Zangmeister, C.D. (2016). Measured wavelength-dependent absorption enhancement of internally mixed black carbon with absorbing and nonabsorbing materials. *Environ. Sci. Technol.* 50: 7982–7990.

Zhai, J., Wang, X., Li, J., Xu, T., Chen, H., Yang, X. and Chen, J. (2015). Thermal desorption single particle mass spectrometry of ambient aerosol in Shanghai. *Atmos. Environ.* 123: 407–414.

Zhang, X., Kim, H., Parworth, C.L., Young, D.E., Zhang, Q., Metcalf, A.R. and Cappa, C.D. (2016). Optical properties of wintertime aerosols from residential wood burning in Fresno, CA: Results from DISCOVER-AQ 2013. *Environ. Sci. Technol.* 50: 1681–1690.

Received for review, November 13, 2017
Revised, April 5, 2018
Accepted, April 13, 2018